

# Monovalent, Clickable, Uncharged, Water-Soluble Perylenediimide-Cored Dendrimers for Target-Specific Fluorescent Biolabeling

Si Kyung Yang,<sup>†</sup> Xinghua Shi,<sup>‡,§,||</sup> Seongjin Park,<sup>‡</sup> Sultan Doganay,<sup>#</sup> Taekjip Ha,<sup>‡,§,||,#</sup> and Steven C. Zimmerman<sup>\*,†</sup>

<sup>†</sup>Department of Chemistry, <sup>‡</sup>Department of Physics, <sup>§</sup>Institute for Genomic Biology, <sup>||</sup>Howard Hughes Medical Institute, and <sup>#</sup>Center for Biophysics and Computational Biology, University of Illinois at Urbana–Champaign, Urbana, Illinois 61801, United States

**S** Supporting Information

**ABSTRACT:** Herein we report the synthesis of water-soluble polyglycerol-dendronized perylenediimides with a single reactive group that undergoes high-yielding click reactions. Single-molecule studies and target-specific biolabeling are reported, including the highly specific labeling of proteins on the surface of living bacterial and mammalian cells.

Fluorescent compounds are useful reporters in biology because they signal their environment and probe a wide range of biological processes, including enzyme catalysis and protein folding and trafficking.<sup>1</sup> The performance of these probes is enhanced when the following criteria are met: (i) high brightness and photostability, (ii) water-solubility, (iii) biocompatibility, and (iv) absorption and emission maxima above 500 nm to minimize the autofluorescence background of cells.<sup>2</sup> In this regard, perylene tetracarboxylic acid diimides (perylene diimides, PDIs) are an attractive class of fluorophores because of their high thermal and photochemical stability with high fluorescence quantum yields in organic solvents.<sup>3</sup> The many successful efforts to prepare soluble and functional PDIs have been reviewed by Langhals, Müllen, Würthner, Nagao, and others.<sup>3,4</sup>

Perhaps the largest challenge with PDI chromophores is developing water-soluble, nonaggregating analogues that retain their exceptional properties. One of the most powerful methods, introduced by Müllen and co-workers, is the incorporation of ionic moieties such as sulfonate, pyridinium, and quaternary ammonium groups into the bay regions of PDI chromophores.<sup>5</sup> The resulting highly charged PDIs are very effective at staining membranes, have the added advantage that the donor groups in the bay region cause a significant red shift in the absorption maximum and an increased Stokes shift, and recently have been prepared with a single reactive group for protein conjugation.<sup>6</sup>

Our interest in developing stable fluorophores for bioimaging led us to seek a neutral and biocompatible PDI for targeted imaging.<sup>7</sup> While this work was in progress, Haag and co-workers reported neutral, water-soluble PDI chromophores prepared by the reaction of amine-cored polyglycerol dendrons (PGDs) and perylene tetracarboxylic acid bisanhydride. The dendritic PDIs exhibited high fluorescence quantum yields in water as a result of reduced aggregation.<sup>8</sup> By combining the advantages of the approaches pioneered by Müllen and Haag, we have prepared neutral PDIs

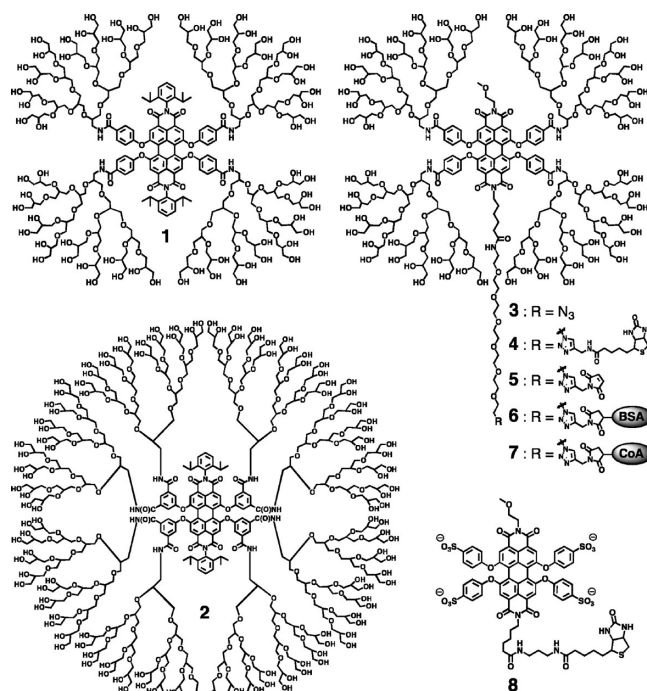


**Figure 1.** Structures of PGD–PDIs 1–7 and PDI 8.

that are bay-substituted with PGDs and contain a single azide group having high reactivity in the click reaction, despite the dense, globular PGD shell.

The key structural feature of the PGD–PDIs reported in this study is a fluorescent PDI core that is linked through amides to four (1 and 3) or eight (2) PGDs, giving 64 and 128 hydroxyl end groups, respectively (Figure 1). PGD–PDIs 1–3 were prepared by HATU-mediated amide coupling of the PDI cores with amine-functionalized PGDs containing eight allyl groups followed by dihydroxylation. The synthetic pathway is described in the Supporting Information (SI). Purification was achieved by a combination of column chromatography, size-exclusion chromatography (SEC), and dialysis, and the purity was determined by analytical SEC, <sup>1</sup>H NMR spectroscopy, and matrix-assisted laser

**Received:** January 29, 2011

**Published:** June 14, 2011

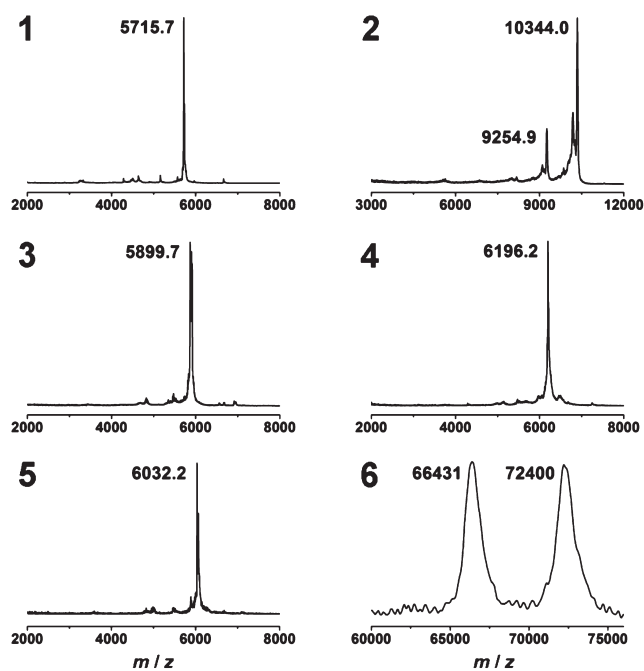


Figure 2. MALDI-TOF mass spectra of PGD-PDIs 1–6.

desorption ionization–time of flight (MALDI-TOF) mass spectrometry. PGD-PDIs 1 and 3 appeared to be homogeneous with a complete attachment of four dendrons in each, while the MALDI-TOF mass spectrum of PGD-PDI 2 revealed a mixture of PDIs having seven and eight attachments, with the latter predominating (Figure 2).

All of the synthesized PGD-PDIs were fully water-soluble and highly fluorescent in water with quantum yields ranging from 0.57 to 0.83. The absorption and emission spectra (Figure 3 and Figure S1 in the SI) showed maxima at 559–569 and 612 nm, respectively, consistent with those of the nondendronized PDI analogues reported in the literature.<sup>5</sup> These results indicate that the attachment of bulky PGDs not only retains the excellent photophysical properties of the original PDI chromophores but also improves their water solubility with minimal aggregation in water, making them useful in bioapplications.

Furthermore, the reactivities of monofunctional PGD-PDI 3 with alkyne-functionalized biotin and maleimide were investigated using click chemistry.<sup>9</sup> Quantitative conversions to PGD-PDIs 4 and 5 containing single biotin and maleimide functions, respectively, were confirmed by comparison of the MALDI mass spectra of 3–5 (Figure 2), demonstrating the potential of our clickable monofunctional PGD-PDIs for conjugation to biomolecules.

The use of copper in the click reaction and the known quenching of fluorescence by metal ions raised the question of whether the fluorescence of the PGD-PDIs might be affected by copper ion. At concentrations higher than those likely to be present from the click reaction, the fluorescence of PGD-PDIs was almost unchanged, whereas that from nondendronized PDI analogues was significantly quenched (see the SI).

To characterize the photostability of PGD-PDIs for single-molecule applications, biotinylated PGD-PDI 4 was immobilized on a PEG-passivated surface through biotin–neutravidin linkages (Figure 4A). This immobilization was indeed highly specific because only negligible binding of 4 was observed in the

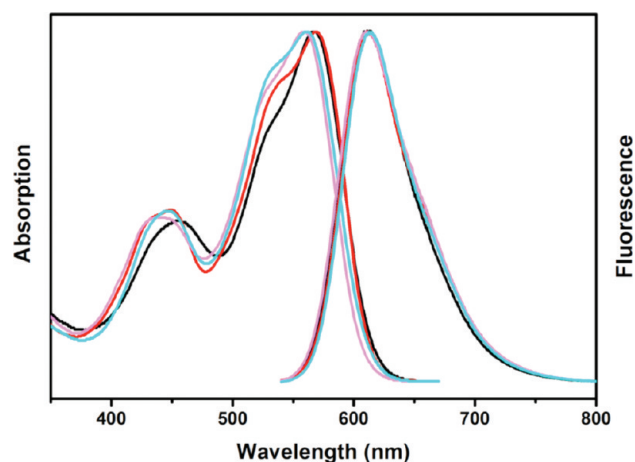


Figure 3. Normalized absorption and emission spectra of PGD-PDIs 1–3 and PDI 8 in water.  $\lambda_{\text{abs,max}}$  (nm),  $\lambda_{\text{em,max}}$  (nm),  $\Phi$  (in water): 567, 612, 0.62 (1, black); 569, 612, 0.83 (2, red); 559, 612, 0.57 (3, pink); 561, 612, 0.39 (8, cyan).

absence of preincubated neutravidin. The optics used were modified from those that are normally implemented in Cy3/Cy5 fluorescence resonance energy transfer (FRET) experiments<sup>10</sup> by removing the dichroic beamsplitter (see the SI). Moreover, this image clearly shows that the fluorescence intensity of single PGD-PDI molecules can easily be distinguished from the background signal with an integration time of 100 ms (Figure 4B). Thus, individual PGD-PDI molecules are bright enough for single-molecule detection under typical imaging conditions.

The intensity time traces of hundreds of isolated molecules were obtained in T50 buffer<sup>10b</sup> containing 10 mM Tris and 50 mM NaCl at pH 8.0 (Figure 4C). As expected, the average intensity of these molecules decayed with time (Figure 4D), and this decay was fit to a single exponential in which the fitted lifetime was defined as the single-molecule photobleaching time,  $\tau_{\text{photobleaching}}$ . From six repeated measurements in different imaging areas,  $\tau_{\text{photobleaching}}$  was determined to be  $9.6 \pm 2.0$  s for 4, while the nondendronized analogue 8 exhibited  $\tau_{\text{photobleaching}} = 7.8 \pm 1.2$  s under the same conditions (see the SI). The fluorescence intensities of single molecules of 4 and 8 were also determined by the average numbers of detected photons as  $21000 \pm 2000$  and  $17000 \pm 2000$  photons, respectively. This result indicates that the original photostability of the PDI can be retained despite substitution with the bulky PGDs.

To illustrate the usefulness of PGD-PDI 4 in targeted biological imaging, the fluorescent labeling of  $\lambda$  receptors on the surface of living bacterial cells using 4 was explored. These receptor proteins, also known as LamB or maltoporin, function as receptors for bacteriophage  $\lambda$  and also facilitate the transport of maltodextrins across the outer membrane of *Escherichia coli*.<sup>11</sup> In vivo, the *E. coli* strain used in this study, called pLO16, produces biotinylated  $\lambda$  receptors with the biotin on the extracellular side.<sup>12</sup> The low efficiency of biotinylation in this strain allowed for the detection of the  $\lambda$ -receptor localization pattern in these cells. As shown in Figure 5A, PGD-PDI 4 produced bright fluorescent spots only at the surfaces of the cells that had been preincubated with streptavidin. Furthermore, in some bacteria, a helical pattern of the spots along the long axis of the bacterium could be discerned, consistent with the surface arrangement of

the proteins.<sup>13</sup> This labeling was highly target-specific, as evidenced by control experiments wherein labeling with 4 in the absence of streptavidin showed no detectable staining of the bacteria cells, either on the surface or inside the bacteria (Figure 5B).

The importance of the dendronized, neutral character of PDI 4 is demonstrated by comparison with nondendronized analogue 8. Although 8 carries a biotin unit, it exhibited only nonspecific staining of bacteria at the same concentration as used for 4 and in the presence of streptavidin. As shown in Figure 5C, cells stained with 8 exhibited a largely homogeneous distribution in fluorescence signal throughout the entire bacterium that could not be removed even after extensive washes. That ionic interactions dominated the cell staining was further shown in experiments

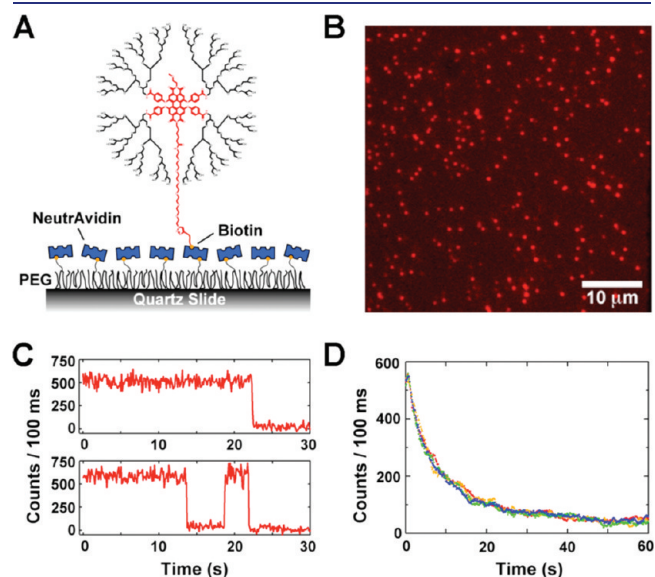


**Figure 4.** Single-molecule analysis of PGD–PDI 4. (A) Experimental scheme, in which 4 was immobilized on a PEG-coated surface through biotin–neutravidin linkages. (B) Fluorescence image of immobilized molecules with pseudo colors. (C) Typical fluorescence intensity time traces of individual molecules in T50 buffer. (D) Average fluorescence intensity as a function of time in T50 buffer.

where 8 was used without preincubation with streptavidin. The cells in this case exhibited a comparable level of staining throughout the bacterium (Figure 5D). These studies demonstrate the importance of the neutral, dendronized PDI in achieving target-specific biolabeling.

To further illustrate the usefulness of PGD–PDIs in targeted biological imaging, fluorescent labeling of ACP-tagged fusion proteins on the surface of living mammalian cells was explored using PGD–PDI 7, which was synthesized by maleimide–thiol coupling between 5 and coenzyme A (CoA). This fusion protein contains a surface-localized glycosylphosphatidylinositol (GPI) anchor upstream of the ACP tag,<sup>14</sup> exposing this tag on the outer surface of the plasma membrane. The ACP tag used here was based on the *E. coli* acyl carrier protein, which can be conjugated to fluorophore derivatives of CoA in the presence of an enzyme named SFP synthase (Figure 6A).<sup>15</sup> As shown in Figure 6B, PGD–PDI 7 clearly produced a bright, surface-localized

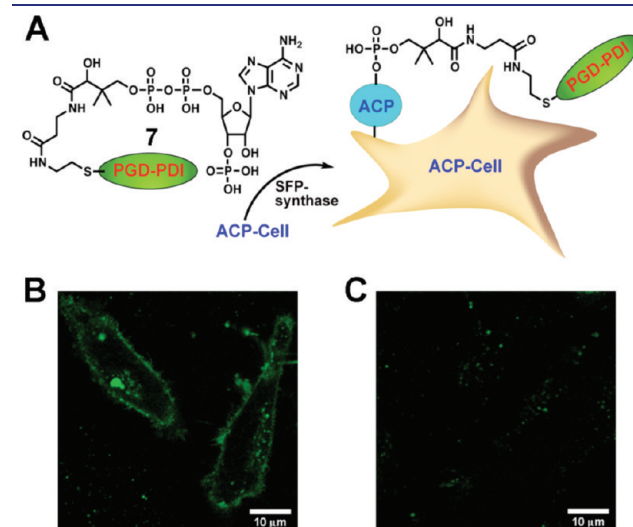


**Figure 6.** Fluorescent labeling of GPI–ACP fusion proteins on the surface of living mammalian cells. (A) Scheme of enzymatic labeling. (B) Fluorescence image of HeLa cells labeled with PGD–PDI 7 after incubation in the presence of SFP synthase. (C) As a control, cells were labeled without SFP synthase.

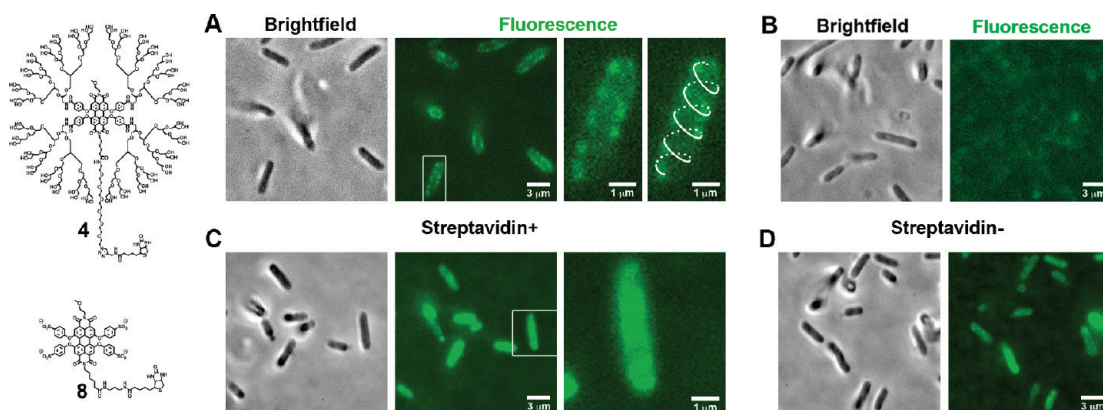


**Figure 5.** Fluorescent labeling of  $\lambda$  receptors on the surface of living bacteria cells. (A) Bright-field and fluorescence images of *E. coli* cells labeled with PGD–PDI 4 after preincubation with streptavidin. The helical pattern of  $\lambda$  receptors is highlighted for one cell in the right panel, which shows an enlargement of the white box in the middle panel. (B) As a control, cells were labeled with 4 in the absence of streptavidin. In (C) and (D), cells were labeled with nondendronized PDI 8 with and without streptavidin preincubation, respectively. All of the images were processed using ImageJ software (NIH), and an intensity range of (10133, 23589) and (28856, 65378) was used for the fluorescence images of 4 and 8, respectively. It should be noted that a scale greater in intensity value was used for 8 because of the higher background and absolute intensity therein.

fluorescence signal on live HeLa cells that had been transiently transfected and incubated with SFP synthase. This labeling was also target-specific, as shown by control experiments in which labeling with **7** in the absence of SFP synthase or transfection with the plasmid encoding the above-mentioned fusion protein showed no apparent fluorescent labeling on the cell surface (Figure 6C and Figure S10).

The methodology for specific protein labeling can be generalized by employing PGD–PDI **5** functionalized with a single maleimide that enables efficient labeling of cysteine residues in proteins in a specific fashion. In this study, **5** was reacted with bovine serum albumin (BSA), which contains a free surface cysteine at amino acid 34, and the formation of PGD–PDI–BSA conjugates was confirmed by the MALDI mass spectrum of **6**, which showed two intense peaks corresponding to native BSA and PGD–PDI **6** at  $m/z$  66 431 and 72 400, respectively (Figure 2). Unreacted BSA was observed because partial oxidation at Cys-34 resulted in only ~50% of the cysteine residues being available for reaction.<sup>16</sup> Quantification using Ellman's assay<sup>17</sup> revealed 46 and ~0% availability of cysteine sites on BSA before and after reaction with PGD–PDI **5**, respectively, indicating quantitative labeling of BSA with **5**. These results demonstrate the versatility of the monofunctional PGD–PDIs for efficient, specific protein labeling.

In conclusion, we have reported the synthesis of a series of highly water-soluble and fluorescent PGD–PDIs and the ability of a clickable monofunctional PGD–PDI to be singly linked to a biomolecule in a specific fashion. Single-molecule and live-bacteria imaging were performed using a single biotinylated PGD–PDI. The key finding was the ability of uncharged, site-isolated PGD–PDIs to serve as highly specific protein labels on the surfaces of living bacteria cells, which is not possible with previous ionic nondendronized PDI analogues. This approach using dendrimers to encapsulate dyes clearly enhances the performance of the dyes and thereby opens up a new generation of biolabels wherein the design would couple a monofunctional fluorescent core with a multivalent periphery containing cellular receptors, therapeutic agents, targeting groups, or ligands.

## ■ ASSOCIATED CONTENT

**S** Supporting Information. Synthetic details, characterization data, experimental procedures, additional data for single-molecule and live-bacteria imaging, and movies (AVI) showing the images acquired at  $z$  positions 1–6 in Figures S4, S6, and S8. This material is available free of charge via the Internet at <http://pubs.acs.org>.

## ■ AUTHOR INFORMATION

**Corresponding Author**  
sczimmer@illinois.edu

## ■ ACKNOWLEDGMENT

We thank the National Institutes of Health and the National Science Foundation for financial support of this research and Kyung Suk Lee for helpful discussions on single-molecule data processing.

## ■ REFERENCES

(1) (a) Giepmans, B. N. G.; Adams, S. R.; Ellisman, M. H.; Tsien, R. Y. *Science* **2006**, *312*, 217. (b) Johnsson, N.; Johnsson, K. *ACS Chem.*

*Biol.* **2007**, *2*, 31. (c) Lavis, L. D.; Raines, R. T. *ACS Chem. Biol.* **2008**, *3*, 142.

(2) (a) Aubin, J. E. *J. Histochem. Cytochem.* **1979**, *27*, 36. (b) Ballou, B.; Ernst, L. A.; Waggoner, A. S. *Curr. Med. Chem.* **2005**, *12*, 795. (c) Kobayashi, H.; Ogawa, M.; Alford, R.; Choyke, P. L.; Urano, Y. *Chem. Rev.* **2010**, *110*, 2620.

(3) (a) Langhals, H. *Chimia* **1994**, *48*, 503. (b) Pasaogullari, N.; Icil, H.; Demuth, M. *Dyes Pigments* **2006**, *69*, 118. (c) Weil, T.; Vosch, T.; Hofkens, J.; Peneva, K.; Müllen, K. *Angew. Chem., Int. Ed.* **2010**, *49*, 9068.

(4) (a) Langhals, H. *Heterocycles* **1995**, *40*, 477. (b) Nagao, Y. *Prog. Org. Coatings* **1997**, *31*, 43. (c) Würthner, F. *Chem. Commun.* **2004**, 1564. (d) Langhals, H. *Helv. Chim. Acta* **2005**, *88*, 1309. (e) Würthner, F. *Pure Appl. Chem.* **2006**, *78*, 2341. (f) Micheli, E.; D'Ambrosio, D.; Franceschin, M.; Savino, M. *Mini-Rev. Med. Chem.* **2009**, *9*, 1622. (g) Avlasevich, Y.; Li, C.; Müllen, K. *J. Mater. Chem.* **2010**, *20*, 3814.

(5) (a) Margineanu, A.; Hofkens, J.; Cotlet, M.; Habuchi, S.; Stefan, A.; Qu, J.; Kohl, C.; Müllen, K.; Vercammen, J.; Engelborghs, Y.; Gensch, T.; De Schryver, F. C. *J. Phys. Chem. B* **2004**, *108*, 12242. (b) Qu, J.; Kohl, C.; Potte, M.; Müllen, K. *Angew. Chem., Int. Ed.* **2004**, *43*, 1528. (c) Kohl, C.; Weil, T.; Qu, J.; Müllen, K. *Chem.—Eur. J.* **2004**, *10*, 5297. (d) Jung, C.; Müller, B. K.; Lamb, D. C.; Nolde, F.; Müllen, K.; Bräuchle, C. *J. Am. Chem. Soc.* **2006**, *128*, 5283.

(6) (a) Abdalla, M. A.; Bayer, J.; Rädler, J. O.; Müllen, K. *Angew. Chem., Int. Ed.* **2004**, *43*, 3967. (b) Peneva, K.; Mihov, G.; Nolde, F.; Rocha, S.; Hotta, J.; Braeckmans, K.; Hofkens, J.; Uji-i, H.; Herrmann, A.; Müllen, K. *Angew. Chem., Int. Ed.* **2008**, *47*, 3372. (c) Peneva, K.; Mihov, G.; Herrmann, A.; Zarrabi, N.; Börsch, M.; Duncan, T. M.; Müllen, K. *J. Am. Chem. Soc.* **2008**, *130*, 5398. (d) Yin, M.; Shen, J.; Pflugfelder, G. O.; Müllen, K. *J. Am. Chem. Soc.* **2008**, *130*, 7806. (e) Yin, M.; Shen, J.; Gropeanu, R. A.; Pflugfelder, G. O.; Weil, T.; Müllen, K. *Small* **2008**, *4*, 894. (f) Cordes, T.; Vogelsang, J.; Anaya, M.; Spagnuolo, C.; Gietl, A.; Summerer, W.; Herrmann, A.; Müllen, K.; Tinnefeld, P. *J. Am. Chem. Soc.* **2010**, *132*, 2404.

(7) Zill, A.; Rutz, A. L.; Kohman, R. E.; Alkilany, A. M.; Murphy, C. J.; Kong, H.; Zimmerman, S. C. *Chem. Commun.* **2011**, 47, 1279.

(8) Heek, T.; Fasting, C.; Rest, C.; Zhang, X.; Würthner, F.; Haag, R. *Chem. Commun.* **2010**, 46, 1884.

(9) Kolb, H. C.; Finn, M. G.; Sharpless, K. B. *Angew. Chem., Int. Ed.* **2001**, *40*, 2004.

(10) (a) Roy, R.; Hohng, S.; Ha, T. *Nat. Methods* **2008**, *5*, 507. (b) Shi, X.; Lim, J.; Ha, T. *Anal. Chem.* **2010**, *82*, 6132.

(11) Boos, W.; Shuman, H. *Microbiol. Mol. Biol. Rev.* **1998**, *62*, 204.

(12) Oddershede, L.; Dreyer, J. K.; Grego, S.; Brown, S.; Berg-Sørensen, K. *Biophys. J.* **2002**, *83*, 3152.

(13) Gibbs, K. A.; Isaac, D. D.; Xu, J.; Hendrix, R. W.; Silhavy, T. J.; Theriot, J. A. *Mol. Microbiol.* **2004**, *53*, 1771.

(14) Eggeling, C.; Ringemann, C.; Medda, R.; Schwarzmann, G.; Sandhoff, K.; Polyakova, S.; Belov, V. N.; Hein, B.; von Middendorff, C.; Schönle, A.; Hell, S. W. *Nature* **2009**, *457*, 1159.

(15) (a) Lambalot, R. H.; Gehring, A. M.; Flugel, R. S.; Zuber, P.; LaCelle, M.; Marahiel, M. A.; Reid, R.; Khosla, C.; Walsh, C. T. *Chem. Biol.* **1996**, *3*, 923. (b) George, N.; Pick, H.; Vogel, H.; Johnsson, N.; Johnsson, K. *J. Am. Chem. Soc.* **2004**, *126*, 8896.

(16) Janatova, J.; Fuller, J. K.; Hunter, M. J. *J. Biol. Chem.* **1968**, *243*, 3612.

(17) Ellman, G. L. *Arch. Biochem. Biophys.* **1959**, *82*, 70.